

Scientific paper

Oxidation of Ruthenium and Iridium Metal by XeF_2 and Crystal Structure Determination of $[\text{Xe}_2\text{F}_3][\text{RuF}_6]\cdot\text{XeF}_2$ and $[\text{Xe}_2\text{F}_3][\text{MF}_6]$ ($\text{M} = \text{Ru}, \text{Ir}$)

Melita Tramšek*, Evgeny Goreshnik and Gašper Tavčar

Jožef Stefan Institute, Jamova 39, SI-1000 Ljubljana, Slovenia

* Corresponding author: E-mail: melita.tramsek@ijs.si

Received: 23-03-2016

Abstract

Salts containing $[\text{Xe}_2\text{F}_3]^+$ cations and $[\text{MF}_6]^-$ anions ($\text{M} = \text{Ru}, \text{Ir}$) were synthesized by the oxidation of metal with excess of XeF_2 in anhydrous hydrogen fluoride (aHF) as a solvent. Single crystals of $[\text{Xe}_2\text{F}_3][\text{RuF}_6]\cdot\text{XeF}_2$, $[\text{Xe}_2\text{F}_3][\text{RuF}_6]$ and $[\text{Xe}_2\text{F}_3][\text{IrF}_6]$ were grown by slow evaporation of the solvent. $[\text{Xe}_2\text{F}_3][\text{RuF}_6]\cdot\text{XeF}_2$ crystallizes in a triclinic $P\bar{1}$ space group ($a = 8.3362(1)$ Å, $b = 8.8197(2)$ Å, $c = 9.3026(4)$ Å; $\alpha = 68.27(1)^\circ$, $\beta = 63.45(1)^\circ$, $\gamma = 82.02^\circ$, $V = 568.09(9)$ Å³ ($Z = 2$)). Discrete $[\text{Xe}_2\text{F}_3]^+$, XeF_2 and $[\text{RuF}_6]^-$ units are found in the asymmetric unit. $[\text{Xe}_2\text{F}_3][\text{RuF}_6]$ and $[\text{Xe}_2\text{F}_3][\text{IrF}_6]$ compounds are isostructural and crystallize in a monoclinic Cc space group ($a = 14.481(3)$ Å (Ru); 14.544(3) Å (Ir); $b = 8.0837(8)$ Å (Ru), 8.0808(7) Å (Ir), $c = 10.952(2)$ Å (Ru), 11.014(2) Å (Ir); $\beta = 136.825(6)^\circ$ (Ru), $139.954(7)^\circ$, $V = 877.2(3)$ Å³ (Ru), 883.6(3) Å³ (Ir); $Z = 4$). The asymmetric unit in the $[\text{Xe}_2\text{F}_3][\text{MF}_6]$ ($\text{M} = \text{Ru}, \text{Ir}$) consists of one $[\text{Xe}_2\text{F}_3]^+$ and one $[\text{MF}_6]^-$ unit.

Keywords: Noble gas fluorides, ruthenium, iridium, crystal structure

1. Introduction

XeF_2 is the most stable and easily handled noble gas fluoride and therefore its chemistry is very extensive. Basic information about XeF_2 , its properties and the possibilities that it offers can be found in review paper and book and the references listed therein.^{1,2} One of its unexpected and interesting abilities is also binding to metal centres in order to form coordination compounds. A large variety of such compounds has been found in previous years.³ The formation of XeF_2 adducts with main-group and transition-metal Lewis acidic pentafluorometalates – MF_5 is known for decades. So far three types of such compounds were found: $2\text{XeF}_2\cdot\text{MF}_5$, $\text{XeF}_2\cdot\text{MF}_5$ and $\text{XeF}_2\cdot(\text{MF}_5)_2$. The degree of ionic character in these compounds varies depending on the Lewis acidity of the respective pentafluoride. Compounds were mainly characterized by vibrational spectroscopy and can be written as salts $[\text{Xe}_2\text{F}_3][\text{MF}_6]$, $[\text{XeF}][\text{MF}_6]$ and $[\text{XeF}][\text{M}_2\text{F}_{11}]$, especially in the case of reactions with strong Lewis acids (for example AsF_5 , SbF_5 , BiF_5 , ...). The formation of 2:1 compounds was found in the cases where M was As, Sb, Bi, Ta, Ru, Os and Ir.^{4,5,6,7} From this type of compounds (2:1 composition) $[\text{Xe}_2\text{F}_3][\text{MF}_6]$ ($\text{M} = \text{As}, \text{Sb}$)^{8,9} were also structurally char-

acterized. The compounds with composition 1:1 ($\text{XeF}^+\text{MF}_6^-$) and 1:2 ($\text{XeF}^+\text{M}_2\text{F}_{11}^-$) were obtained for the most of the MF_5 mentioned above. Some of them were structurally characterized: $[\text{XeF}][\text{MF}_6]$ ($\text{M} = \text{As}, \text{Sb}, \text{Bi}, \text{Ru}$ and Ir)^{10,11,12,13} and $[\text{XeF}][\text{M}_2\text{F}_{11}]$ ($\text{M} = \text{Sb}, \text{Bi}$).¹¹ One of the latest structurally characterized examples is also and $[\text{XeF}][\text{IrSbF}_{11}]$ with two different metals in the anion.¹³ $[\text{Xe}_2\text{F}_3]^+$ and $[\text{XeF}]^+$ cations were recently found with nonoctahedral anion in the xenon(II) polyfluorodotitanates(IV): $[\text{Xe}_2\text{F}_3][\text{Ti}_8\text{F}_{33}]$ and $[\text{XeF}][\text{Ti}_9\text{F}_{38}]$.¹⁴

The present study reports about the synthesis and structural characterization of three noble gas salts containing $[\text{Xe}_2\text{F}_3]^+$ cation: $[\text{Xe}_2\text{F}_3][\text{RuF}_6]\cdot\text{XeF}_2$, $[\text{Xe}_2\text{F}_3][\text{RuF}_6]$ and $[\text{Xe}_2\text{F}_3][\text{IrF}_6]$.

2. Experimental

2.1. General Experimental Procedure and Reagents

Volatile materials (anhydrous HF, F_2) were handled in an all PTFE vacuum line equipped with PTFE (polyte-

trafluoroethylene) valves. The manipulations of the non-volatile materials were carried out in a glove-box (M. Braun). The residual water in the atmosphere within the glove-box never exceeded 1 ppm. The reactions were carried out in FEP (tetrafluoroethylene-hexafluoropropylene; Polytetra GmbH, Germany) reaction vessels (height 250–300 mm with inner diameter 16 mm and outer diameter 19 mm) equipped with PTFE valves and PTFE coated stirring bars. T-shaped reaction vessels from PTFE, which were constructed as described earlier, were used for the crystallization process.¹⁵ Prior to their use all reaction vessels were passivated with elemental fluorine. Fluorine was used as supplied (Solvay Fluor and Derivate GmbH, Germany). Anhydrous HF (Linde, 99.995%) was treated with K_2NiF_6 (Advance Research Chemicals, Inc.) for several hours prior to use. XeF_2 was synthesized by photochemical reaction between Xe and F_2 .¹⁶ **Caution:** *aHF, F_2 and XeF_2 must be handled with great care in a well-ventilated fume hood, and protective gear must be worn at all times.*

2. 2. Synthesis and Characterization Procedures

Synthetic procedures for the ruthenium and iridium compounds were the same. Metal powder (Ru: 0.215 g, 2.13 mmol, Ir: 0.430 g, 2.20 mmol) was added into a reaction vessel inside the glove-box. The aHF was condensed into the reaction vessel at $-196\text{ }^\circ\text{C}$ at the vacuum line. Large excess of XeF_2 (mole ratio M : XeF_2 was approximately 1:10) was weighed into another reaction vessel inside the glove-box. Anhydrous HF was added to the XeF_2 and the reaction vessel was warmed up to room temperature. These two reaction vessels (one with the suspension of the metal, and another with dissolved XeF_2) were attached in a T-shape manner and additional valve was used in order to provide completely closed system. The XeF_2 solution was then poured into cold reaction vessel ($-196\text{ }^\circ\text{C}$) with suspension of the metal powder (Ru, Ir). The reaction vessel was left to slowly warm up to room temperature. The solution turned immediately green in the case of ruthenium but the reaction with iridium proceeded at room temperature for several days (light gray solid product). Products of the oxidation were isolated by removal of aHF and excessive XeF_2 under dynamic vacuum at room temperature. Several crystallization experiments were performed. In some cases the product of the oxidation of the metal with XeF_2 was dissolved in aHF in a wider arm of the T-shaped crystallization vessel, while in the other additional XeF_2 was added. Solution was then poured into narrow arm of the crystallization vessel and left to crystallize by a small temperature gradient used for slow evaporation of aHF.

The Raman spectra were recorded at room temperature with a Horiba Jobin Yvon LabRam-HR spectrometer equipped with an Olympus BXFM-ILHS microscope and

CCD detector. The samples were excited by the 632.8 nm emission line of a He-Ne laser. Samples for measurement were transferred into the quartz capillary inside glove-box.

The crystallographic parameters and summaries of data collection for all compounds are presented in Table 1. Single-crystal data were collected on a Rigaku AFC7 diffractometer using graphite monochromatized $MoK\alpha$ radiation at 200 K. Crystals were immersed into perfluorinated oil in glove-box and further on selected under the microscope. An empirical multi-scan absorption correction was applied. All structures were solved by direct methods using SIR-92¹⁷ and SHELXS-97 programs (teXan crystallographic software package of Molecular Structure Corporation)¹⁸ and refined with SHELXL-97 software,¹⁹ implemented in program package WinGX.²⁰ Full-matrix least-squares refinements based on F^2 were carried out for the positional and thermal parameters for all non-hydrogen atoms. The figures were prepared using DIAMOND 3.1 software.²¹ Further details of the crystal-structure investigation may be obtained from the Fachinformationszentrum Karlsruhe, 76344 Eggenstein-Leopoldshafen, Germany, on quoting the depository number: CSD-430805 for $[Xe_2F_3][RuF_6]$, CSD-430806 for $[Xe_2F_3][IrF_6]$ and CSD-430807 for $[Xe_2F_3][RuF_6]\cdot XeF_2$, respectively.

3. Results and Discussion

The oxidation power of XeF_2 was used in order to prepare previously mentioned Ru(V) and Ir(V) compounds. XeF_2 dissolved in anhydrous hydrogen fluoride (aHF) was also used as selective inorganic fluorinating reagent for oxidation and fluorination of Ir and RuF_3 almost three decades ago with final products being IrF_5 and RuF_5 .²² Ruthenium metal was oxidized rapidly with vigorous reaction being observed during the warming of the reaction vessel from $-196\text{ }^\circ\text{C}$ to room temperature. A clear, slightly green solution was obtained. We used a slightly modified procedure for the preparation of the ruthenium compound ($[Xe_2F_3][MF_6]\cdot XeF_2$). The product was further used for the synthesis of $[Ba(XeF_2)_5][RuF_6]$.²³ The same reaction with iridium proceeded for several weeks. The colour of the solution was red-brown at the beginning and after several days became slightly yellow with some grey precipitate – same as the solid product after its isolation. The grey solid obtained by the oxidation of Ir metal with XeF_2 was re-dissolved in aHF and a clear, slightly green solution was obtained. Products of the reactions were also monitored by Raman spectroscopy, which shows (Figure 1) that in both cases the compound with composition $[Xe_2F_3][MF_6]\cdot nXeF_2$ (M = Ru, Ir, n is approx. 1 according to the mass balance of the reaction) were obtained. An alternative method used for the preparation of related compounds with Ru(V) ($KRuF_6$, $LiRuF_6$) and Ir(V) ($KIrF_6$, $LiIrF_6$) with al-

kaline metals is the room temperature oxidation with elemental fluorine in the presence of Lewis base (KF) in aHF.^{24,25} One of the recently published ways to prepare soluble iridium compounds, which seems to be important for modern “urban mining”, is the reaction of the metal with tetrafluorobromates (MBrF₄; M = K, Rb, Cs).²⁶

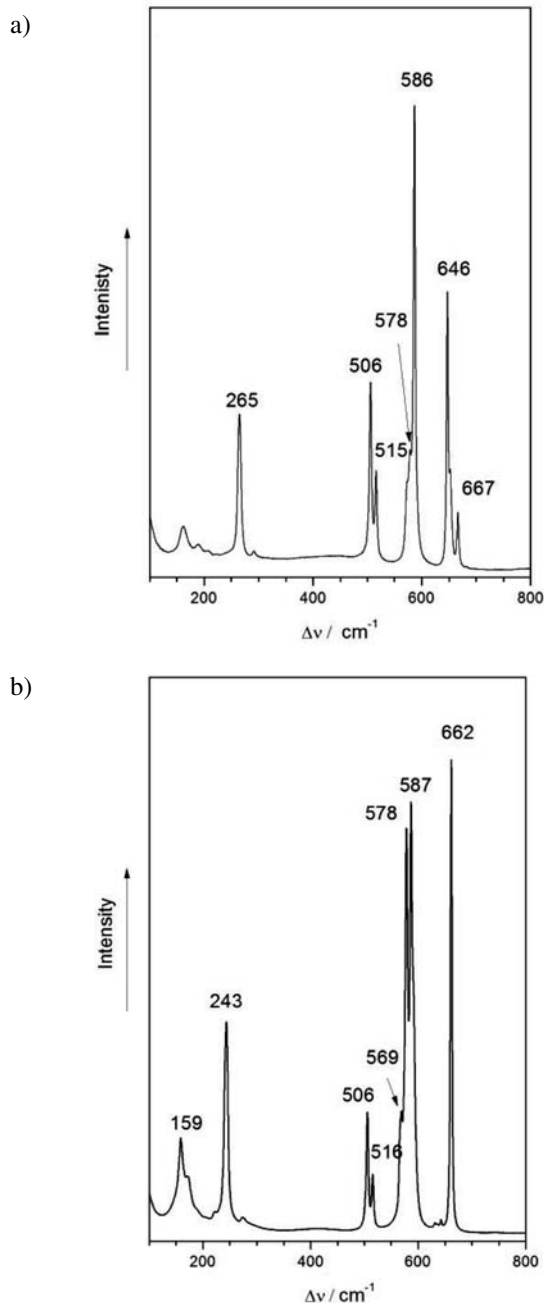


Figure 1. Raman spectra of $[\text{Xe}_2\text{F}_3][\text{RuF}_6]\cdot\text{XeF}_2$ (a) and $[\text{Xe}_2\text{F}_3][\text{IrF}_6]\cdot\text{XeF}_2$ (b)

For solid XeF_2 the band at 497 cm^{-1} is characteristic.²⁷ The bands at 506 cm^{-1} , 515 cm^{-1} in ruthenium compound and 506 cm^{-1} and 516 cm^{-1} in iridium compound can be attributed to the XeF_2 weakly associated with

$[\text{Xe}_2\text{F}_3]^+$ cations and $[\text{MF}_6]^-$ anions in the $[\text{Xe}_2\text{F}_3][\text{MF}_6]\cdot\text{XeF}_2$ product. Similar positions and assignment of these bands were observed in some other cases in the system $\text{XeF}_2\text{-MF}_5$ (M = Sb, Ta, Nb). The weakly associated XeF_2 was found in the melt of the compounds.²⁸ “Free” XeF_2 was also found in the compounds $\text{XeF}_2\cdot\text{XeF}_6\cdot\text{AsF}_5$ and $\text{XeF}_2\cdot 2(\text{XeF}_6)\cdot 2(\text{AsF}_5)$, where the Raman bands depend on the interaction of the so called “free” XeF_2 molecule with cations and anions and consequential distortion of its shape. “Free” XeF_2 in $\text{XeF}_2\cdot 2(\text{XeF}_6)\cdot 2(\text{AsF}_5)$ is probably in a completely symmetric environment, therefore the band assigned to it coincides with the symmetric stretching frequency in molecular XeF_2 (497 cm^{-1}). On the other hand Raman spectrum of $\text{XeF}_2\cdot\text{XeF}_6\cdot\text{AsF}_5$ doesn’t show a symmetric vibration of molecular XeF_2 but two bands at 557 cm^{-1} and 429 cm^{-1} which represent a distorted XeF_2 molecule meaning that XeF_2 in this compound can be far from “free”.²⁹ Linear distortion of XeF_2 was found also in the Raman spectrum of $\text{XeF}_2\cdot[\text{XeF}_5][\text{RuF}_6]$.³⁰ Bands at 578 cm^{-1} and 586 cm^{-1} in the ruthenium compound and bands at 578 cm^{-1} and 587 cm^{-1} in iridium compound can be confidently assigned to the Xe-F_l stretch vibrations of the $[\text{Xe}_2\text{F}_3]^+$ cation. They are in the region that is characteristic for such vibrations (from ca. 575 cm^{-1} to 600 cm^{-1}). The bands at 646 cm^{-1} , 667 cm^{-1} and 265 cm^{-1} for the ruthenium compound and 662 cm^{-1} and 243 cm^{-1} for the iridium can be assigned to the vibration of the $[\text{MF}_6]^-$ anions. Products with additional XeF_2 are not stable under

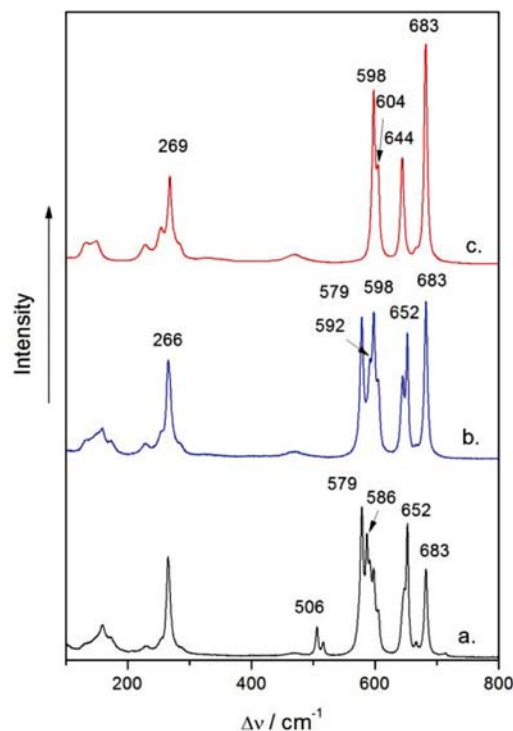


Figure 2. Raman spectra of the reaction mixture during the isolation of ruthenium compound on the vacuum system: a.) mixture of $[\text{Xe}_2\text{F}_3][\text{RuF}_6]\cdot\text{XeF}_2$, $[\text{Xe}_2\text{F}_3][\text{RuF}_6]$ and $[\text{XeF}][\text{RuF}_6]$; b.) mixture of $[\text{Xe}_2\text{F}_3][\text{RuF}_6]$ and $[\text{XeF}][\text{RuF}_6]$; c.) $[\text{XeF}][\text{RuF}_6]$.

dynamic vacuum at room temperature. They release XeF_2 , which leads to the formation of the $[\text{Xe}_2\text{F}_3][\text{MF}_6]$ and further on to the $[\text{XeF}][\text{MF}_6]$ ($M = \text{Ru}, \text{Ir}$) compounds. According to the mass balance of the reactions and Raman spectra, the $[\text{XeF}][\text{MF}_6]$ ($M = \text{Ru}, \text{Ir}$) salts seem to be stable at room temperature under dynamic vacuum. Raman analysis of the slow removal of XeF_2 under dynamic vacuum in the case of ruthenium is shown in Figure 2. In the spectrum shown on the Figure 2a (black colour) all three phases can be found: $[\text{Xe}_2\text{F}_3][\text{RuF}_6]\cdot\text{XeF}_2$, $[\text{Xe}_2\text{F}_3][\text{RuF}_6]$ and $[\text{XeF}][\text{RuF}_6]$. With the release of the XeF_2 , phases $[\text{Xe}_2\text{F}_3][\text{RuF}_6]$ and $[\text{XeF}][\text{RuF}_6]$ are found (Figure 2b (blue colour)). Prolonged pumping on the vacuum system (overnight) ended up with $[\text{XeF}][\text{RuF}_6]$ as the only product. Position and the intensities of the bands for $[\text{Xe}_2\text{F}_3][\text{RuF}_6]$ and $[\text{XeF}][\text{RuF}_6]$ are in the agreement with those published previously.⁴

3. 1. Crystal Structure Determination of $[\text{Xe}_2\text{F}_3][\text{RuF}_6]\cdot\text{XeF}_2$ and $[\text{Xe}_2\text{F}_3][\text{MF}_6]$ ($M = \text{Ru}, \text{Ir}$)

Three compounds in this system were structurally characterized. Summary of crystal data and refinement re-

sults for $[\text{Xe}_2\text{F}_3][\text{RuF}_6]\cdot\text{XeF}_2$ and $[\text{Xe}_2\text{F}_3][\text{MF}_6]$ ($M = \text{Ru}, \text{Ir}$) are presented in Table 1 and selected distances and angles are found in Table 2. Several unsuccessful attempts were made in order to prepare suitable single crystals of the $[\text{Xe}_2\text{F}_3][\text{IrF}_6]\cdot\text{XeF}_2$. So far we were only able to resolve the structure of $[\text{Xe}_2\text{F}_3][\text{IrF}_6]$.

The structure of $[\text{Xe}_2\text{F}_3][\text{RuF}_6]\cdot\text{XeF}_2$ consists of discrete $[\text{Xe}_2\text{F}_3]^+$, XeF_2 and $[\text{RuF}_6]^-$ units (Figure 3). XeF_2 molecules and $[\text{Xe}_2\text{F}_3]^+$ cations are oriented roughly perpendicularly to each other. When viewed along $(-3 -4 3)$ direction alternating cationic and anionic layers could be seen. Anions are separated by XeF_2 molecules (Figure 4). The compound is structurally related to $[\text{Kr}_2\text{F}_3][\text{SbF}_6]\cdot\text{KrF}_2$ in which the crystal packing consists of alternating cation and equally populated anion/ KrF_2 layers.³¹

XeF_2 molecules are nearly linear with distances being 1.980(7) and 1.992(7) Å and angle F10-Xe-F11 of 178.9(4)°. $[\text{Xe}_2\text{F}_3]^+$ cation exhibit a planar, V shape configuration with nearly symmetrical Xe-F_t bonds (2.139(7) and 2.152(7) Å) and a Xe-F_b-Xe angle of 154.3(4)°. The $[\text{RuF}_6]^-$ anions are slightly distorted octahedra with Ru-F bond distances in the range from 1.834(8) to 1.861(7) Å.

Table 1. Crystal data and structure refinement for $[\text{Xe}_2\text{F}_3][\text{RuF}_6]\cdot\text{XeF}_2$ and $\text{Xe}_2\text{F}_3\text{MF}_6$ ($M = \text{Ru}, \text{Ir}$)

	$[\text{Xe}_2\text{F}_3][\text{RuF}_6]\cdot\text{XeF}_2$	$[\text{Xe}_2\text{F}_3][\text{RuF}_6]$	$[\text{Xe}_2\text{F}_3][\text{IrF}_6]$
Empirical formula	$\text{RuXe}_3\text{F}_{11}$	RuXe_2F_9	IrXe_2F_9
Formula weight	703.94	534.67	625.8
Wavelength, MoK α	0.71069 Å	0.71069 Å	0.71069 Å
Crystal system,			
Space group	triclinic	monoclinic	monoclinic
	<i>P</i> -1	<i>Cc</i>	<i>Cc</i>
Temperature, K	200	200	200
Unit cell dimensions			
<i>a</i> , Å	8.3362(1)	14.481(3)	14.544(3)
<i>b</i> , Å	8.8197(2)	8.0837(8)	8.0808(7)
<i>c</i> , Å	9.3026(4)	10.952(2)	11.014(2)
α , °	68.27(1)	90	90
β , °	63.45(1)	136.825(6)	136.954(7)
γ , °	82.02(2)	90	90
<i>V</i> , Å ³	568.09(9)	877.2(3)	883.6(3)
<i>Z</i>	2	4	4
Calculated density, g/cm ³	4.115	4.048	4.704
Absorption coeff., mm ⁻¹	10.289	9.477	22.745
<i>F</i> (000)	610	932	1064
Crystal size, mm	0.08×0.06×0.04	0.10×0.10×0.08	0.10×0.07×0.05
Colour	colourless	colourless	colourless
Theta range for data collection, deg	2.487–28.6986	3.2522–28.5637	3.1256–27.9323
Limiting indices	$-8 \leq h \leq 11, -10 \leq k \leq 11, -11 \leq l \leq 12$	$-18 \leq h \leq 16, -10 \leq k \leq 10, -8 \leq l \leq 14$	$-18 \leq h \leq 17, -6 \leq k \leq 10, -6 \leq l \leq 14$
Measured reflections	2259	1174	1129
Used in refinement	1837	890	1074
Free parameters	137	111	111
Goodness-of-fit on <i>F</i> ²	1.134	1.134	1.067
<i>R</i> indices	<i>R</i> ₁ = 0.0608 <i>wR</i> ₁ = 0.1775	<i>R</i> ₁ = 0.0371 <i>wR</i> ₁ = 0.0849	<i>R</i> ₁ = 0.0382 <i>wR</i> ₁ = 0.0963
Largest diff. peak and hole, e Å ⁻³	1.758 and -3.063	1.579 and -1.236	1.699 and -2.329

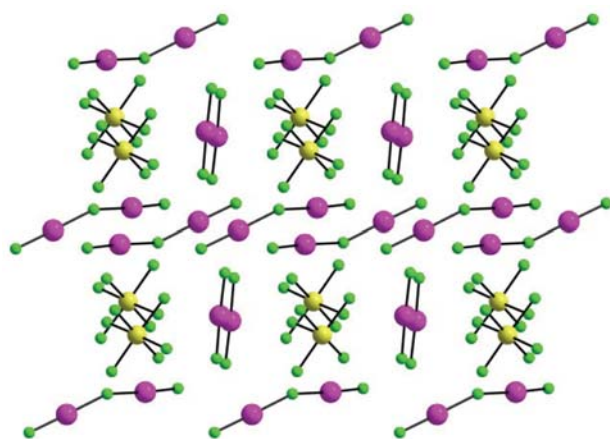
Table 2. Selected distances (Å) and angles (°) in $[\text{Xe}_2\text{F}_3][\text{RuF}_6] \cdot \text{XeF}_2$, $[\text{Xe}_2\text{F}_3][\text{MF}_6]$ (M = Ru, Ir)

	$[\text{Xe}_2\text{F}_3][\text{RuF}_6] \cdot \text{XeF}_2$	$[\text{Xe}_2\text{F}_3][\text{RuF}_6]$	$[\text{Xe}_2\text{F}_3][\text{IrF}_6]$
Xe1-F1	2.139(7)	2.09(1)	2.12(2)
Xe2-F1	2.152(7)	2.17(1)	2.15(2)
Xe1-F2	1.913(8)	1.90(2)	1.88(2)
Xe2-F3	1.919(6)	1.92(2)	1.96(2)
Xe3-F10	1.980(7)		
Xe3-F11	1.992(7)		
Xe1-F1-Xe2	154.3(4)	161.5(5)	161.3(8)
F10-Xe3-F11	178.9(4)		

Figure 3. Asymmetric unit in $[\text{Xe}_2\text{F}_3][\text{RuF}_6] \cdot \text{XeF}_2$ with thermal ellipsoids drawn at 50 % probability level.

The Xe centres from both XeF_2 and $[\text{Xe}_2\text{F}_3]^+$ moieties interact with fluorine atoms from another structural units. The shortest F9...Xe2ⁱⁱⁱ and F9...Xe1 distances of 3.190(7) and 3.216(7) Å respectively correspond to slightly elongated Ru1-F9 bond (1.861(7) Å). There are four XeF_2 molecules bound to one anion *via* Xe...F contacts of 3.301(7)–3.373(7) Å. Terminal F2 and F3 atoms from each $[\text{Xe}_2\text{F}_3]^+$ also form longer contacts with Xe centres from other cations. These contacts are slightly longer (from 3.219(7) to 3.278(8) Å, correspondingly) than those in the case of XeF_2 molecules.

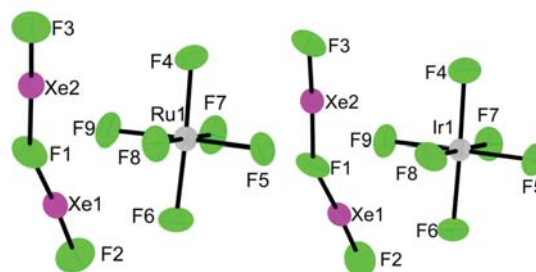
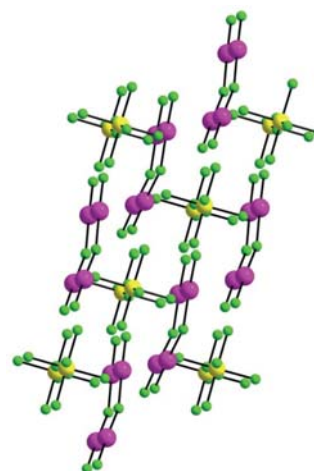
Weak Xe...F(Xe) and Xe...F(Ru) interactions connect above mentioned units into three-dimensional network (Figure 4) if contacts shorter than 3.4 Å are taken into consideration. The sum of the van der Waals radius for xenon (2.16 Å) and fluorine (1.35 Å) is 3.51 Å.³²

**Figure 4.** Packing diagram of $[\text{Xe}_2\text{F}_3][\text{RuF}_6] \cdot \text{XeF}_2$.

The $[\text{Xe}_2\text{F}_3][\text{MF}_6]$ (M = Ru, Ir) salts are both isostructural with monoclinic $[\text{Xe}_2\text{F}_3][\text{SbF}_6]$.⁹ Asymmetrical unit in both cases consists of one $[\text{Xe}_2\text{F}_3]^+$ cation and one $[\text{MF}_6]^-$ anion (Figure 5). In both cases sev-

eral Xe...F contacts in the range above 3 Å can be found. A packing diagram along the *b*-axis is presented in Figure 6. A less bent structure of the $[\text{Xe}_2\text{F}_3]^+$ cation is found in the case of $[\text{Xe}_2\text{F}_3][\text{MF}_6]$ (M = Ru, Ir) compared to the $[\text{Xe}_2\text{F}_3][\text{RuF}_6] \cdot \text{XeF}_2$. The Xe...F_b...Xe angle is 161.5(5)° in the ruthenium compound and 161.3(8)° in the iridium compound. These angles are in agreement with those in isostructural monoclinic $[\text{Xe}_2\text{F}_3][\text{SbF}_6]$ (Xe...F_b...Xe = 160.3°). Bridging angle of Xe...F_b...Xe in $[\text{Xe}_2\text{F}_3]^+$ cations vary from 139.8° as observed in trigonal $[\text{Xe}_2\text{F}_3][\text{AsF}_6]$ ⁹ to the widest one being 164.3° as observed in $[\text{Xe}_2\text{F}_3][\text{Ti}_8\text{F}_{33}]$.¹⁴

Strong dependence of the Xe...F_b...Xe bridge angle on the crystal packing and on the nature of the counter anion was demonstrated in a previous study. Calculation (Christiansen-Ermler ECP) in the same study also predicted non-linear structure of the $[\text{Xe}_2\text{F}_3]^+$ cation with a bridging angle of 168°.⁹

**Figure 5.** Asymmetric units in $[\text{Xe}_2\text{F}_3][\text{RuF}_6]$ and $[\text{Xe}_2\text{F}_3][\text{IrF}_6]$ with thermal ellipsoids drawn at 50 % probability level.**Figure 6.** Packing diagram of $[\text{Xe}_2\text{F}_3][\text{RuF}_6]$ along *b*-axis.

4. Conclusions

The oxidizing power of XeF_2 was demonstrated by oxidation of ruthenium and iridium metal in aHF as a solvent. Products of the oxidation belong to the family of no-

ble gas compounds with $[\text{Xe}_2\text{F}_3]^+$ cations. Salt with composition $[\text{Xe}_2\text{F}_3][\text{RuF}_6] \cdot \text{XeF}_2$ was structurally characterized. The synthesis and characterization with Raman spectroscopy of the new salt $[\text{Xe}_2\text{F}_3][\text{IrF}_6] \cdot \text{XeF}_2$ are also reported. Single crystal structures of $[\text{Xe}_2\text{F}_3][\text{RuF}_6]$ and $[\text{Xe}_2\text{F}_3][\text{IrF}_6]$ were determined.

5. Acknowledgement

The authors gratefully acknowledge the Slovenian Research Agency (ARRS) for financial support of the Research Program P1-0045 (Inorganic Chemistry and Technology).

6. References

1. M. Tramšek, B. Žemva, *Acta Chim. Slov.* **2006**, *53*, 105–116.
2. J. Reedjik, K. Poepplmeier (Ed.): *Comprehensive Inorganic Chemistry II*, Elsevier, Oxford, **2013**, D. S. Brock, G. J. Schrobilgen, B. Žemva, Vol. 1, pp755–822
3. M. Tramšek, G. Tavčar, *J. Fluorine Chem.* **2015**, *174*, 14–21. <http://dx.doi.org/10.1016/j.jfluchem.2014.08.009>
4. F. O. Sladky, P. A. Bulliner, N. Bartlett, *J. Chem. Soc.* **1969**, 2179–2188. <http://dx.doi.org/10.1039/J19690002179>
5. B. Frlec, J. H. Holloway, *J. Chem. Soc.* **1975**, 535–540.
6. J. Gillespie, D. Martin, G. J. Schrobilgen, *J. Chem. Soc. Dalton* **1980**, 1898–1903.
7. J. H. Holloway, J. G. Knowles, *J. Chem. Soc.* **1969**, 756–761. <http://dx.doi.org/10.1039/j19690000756>
8. N. Bartlett, B. G. DeBoer, F. J. Hollander, F. O. Sladky, D. H. Templeton, A. Zalkin, *Inorg. Chem.* **1974**, *13*, 780–785. <http://dx.doi.org/10.1021/ic50134a004>
9. B. A. Fir, M. Gerken, B. E. Pointner, H. P. A. Mercier, D. A. Dixon, G. J. Schrobilgen, *J. Fluorine Chem.* **2000**, *105*, 159–167. [http://dx.doi.org/10.1016/S0022-1139\(00\)00306-7](http://dx.doi.org/10.1016/S0022-1139(00)00306-7)
10. A. Zalkin, D. L. Ward, R. N. Biagoni, D. H. Templeton, N. Bartlett, *Inorg. Chem.* **1978**, *17*, 1318–1322. <http://dx.doi.org/10.1021/ic50183a044>
11. H. St. A. Elliot, J. F. Lehman, H. P. A. Mercier, H. D. B. Jenkins, G. J. Schrobilgen, *Inorg. Chem.* **2010**, *49*, 8504–8523.
12. N. Bartlett, M. Gennis, D. D. Gibler, B. K. Morrell, A. Zalkin, *Inorg. Chem.* **1973**, *12*, 1717–1721. <http://dx.doi.org/10.1021/ic50126a002>
13. F. Tamadon, S. Seidel, K. Seppelt, *Acta Chim. Slov.* **2013**, *60*, 491–494.
14. K. Radan, E. Goresnik, B. Žemva, *Agew. Chem. Int. Ed.* **2014**, *53*, 13715–13719.
15. M. Lozinšek, E. Goresnik, B. Žemva, *Acta Chim. Slov.* **2014**, *61*, 542–547.
16. R. N. Grimes (Ed.). *Inorganic Syntheses*, John Wiley, New York, **1992**, A. Šmalc, K. Lutar, Vol. 29, pp. 1–4.
17. A. Altomare, M. Cascarano, M., C. Giacovazzo, A. Guagliardi, *J. Appl. Cryst.* **1993**, *26*, 343–350. <http://dx.doi.org/10.1107/S0021889892010331>
18. Molecular Structure Corporation. (1997–1999), teXsan for Windows, Single Crystal Structure Analysis Software. Version 1.06, MSC, 9009 New Trails Drive, The Woodlands, TX 77381, USA.
19. G. M. Sheldrick, *Acta Cryst.* **2008**, *A64*, 112–122. <http://dx.doi.org/10.1107/S0108767307043930>
20. L. J. Farrugia, *J. Appl. Cryst.* **1999**, *32*, 837–838. <http://dx.doi.org/10.1107/S0021889899006020>
21. DIAMOND v3.1, Crystal Impact GbR, Bonn, Germany, 2004–2005
22. R. C. Burns, I. D. MacLeod, T. A. O'Donnell, T. E. Peel, K. A. Philips, A. B. Waugh, *J. Inorg. Nucl. Chem.* **1977**, *39*, 1737–1739. [http://dx.doi.org/10.1016/0022-1902\(77\)80193-0](http://dx.doi.org/10.1016/0022-1902(77)80193-0)
23. T. Bunič, M. Tramšek, E. Goresnik, B. Žemva, *Collect. Czech. Chem. Commun.* **2008**, *73*, 1645–1654. <http://dx.doi.org/10.1135/cccc20081645>
24. G. Lucier, S. H. Elder, L. Chacón, N. Bartlett, *Eur. J. Solid State Inorg. Chem.* **1996**, *33*, 809–820.
25. G. Tavčar, B. Žemva, *Inorg. Chem.* **2013**, *52*, 4139–4323. <http://dx.doi.org/10.1021/ic302323j>
26. S. Ivlev, P. Woidy, F. Kraus, I. Gerin, R. Ostvald, *Eur. J. Inorg. Chem.* **2013**, 4984–4987. <http://onlinelibrary.wiley.com/doi/10.1002/ejic.201300618/abstract>
27. P. A. Agron, G. M. Begun, H. A. Levy, A. A. Mason, C. G. Jones, D. F. Smith, *Science* **1963**, *139*, 842–844. <http://dx.doi.org/10.1126/science.139.3557.842>
28. B. Frlec, J. H. Holloway, *J. Inorg. Nucl. Chem. Supplement I* **1976**, *28*, 167–171.
29. N. Bartlett, M. Wechsberg, *Z. anorg. Allg. Chem.* **1971**, 385, 5–17. <http://dx.doi.org/10.1002/zaac.19713850103>
30. B. Žemva, L. Golič, J. Slivnik, *Vestn. Slov. Kem. Druš.* **1983**, *30*, 365–376.
31. J. F. Lehman, D. A. Dixon, G. J. Schrobilgen, *Inorg. Chem.* **2001**, *40*, 3002–3017. <http://dx.doi.org/10.1021/ic001167w>
32. A. Bondi, *J. Phys. Chem.* **1964**, *68*, 441–451. <http://dx.doi.org/10.1021/j100785a001>

Povzetek

Z oksidacijo kovine (Ru, Ir) s presežnim XeF₂ v brezvodnem vodikovem fluoridu (aHF) kot topilu smo pripravili spojine s kationi [Xe₂F₃]⁺ in anioni [MF₆]⁻ (M = Ru, Ir). Kristale [Xe₂F₃][RuF₆] · XeF₂, [Xe₂F₃][RuF₆] in [Xe₂F₃][IrF₆], ki so bili primerni za rentgensko strukturno analizo, smo pripravili s počasnim izhlapevanjem topila. [Xe₂F₃][RuF₆] · XeF₂ kristalizira v triklinskem kristalnem sistemu; prostorska skupina *P*-1 (*a* = 8,3362(1) Å, *b* = 8,8197(2) Å, *c* = 9,3026(4) Å; *α* = 68,27(1)°, *β* = 63,45(1)°, *γ* = 82,02°, *V* = 568,09(9) Å³ (*Z* = 2)). V asimetrični enoti spojine se nahajajo [Xe₂F₃]⁺, XeF₂ in [RuF₆]⁻. Spojini [Xe₂F₃][RuF₆] in [Xe₂F₃][IrF₆] sta izostrukturni in kristalizirata v monoklinskem kristalnem sistemu; prostorska skupina *Cc* (*a* = 14,481(3) Å (Ru); 14,544(3) Å (Ir); *b* = 8,0837(8) Å (Ru), 8,0808(7) Å (Ir), *c* = 10,952(2) Å (Ru), 11,014(2) Å (Ir); *β* = 136,825(6)° (Ru), 139,954(7)°, *V* = 877,2(3) Å³ (Ru), 883,6(3) Å³ (Ir); *Z* = 4). Asimetrični enota [Xe₂F₃][MF₆] (M = Ru, Ir) je sestavljena iz [Xe₂F₃]⁺ in [MF₆]⁻ ionov.